

---

# Higher-order interpolation for mesh adaptation

Estelle Mbinky<sup>1</sup>, Frédéric Alauzet<sup>1</sup>, and Adrien Loseille<sup>1</sup>

INRIA, Gamma Project, Rocquencourt, BP 105, 78153 Le Chesnay Cedex, France  
{Estelle.Mbinky, Frederic.Alauzet, Adrien.Loseille}@inria.fr

**Summary.** This paper addresses the construction of anisotropic metrics from higher-order interpolation error in 2 dimensions [2, 3] for mesh adaptation. Our approach is based on homogeneous polynomials that model a local interpolation error. Optimal orientation and ratios are found by using the Sylvester decomposition [4]. Then we apply a global calculus of variation to get the optimal metric field minimizing the  $\mathbf{L}^p$  norm of the interpolation error. We illustrate this approach on a numerical example.

## 1 Third order interpolation error model

We define the quadratic interpolate  $\Pi_h^2 u$  of  $u$  on a mesh  $\mathcal{H}$  by:

$$\forall \mathbf{x} \in \Omega, \quad \Pi_h^2 u(\mathbf{x}) = \sum_{i=1}^6 u(\mathbf{p}_i) \varphi_i(\mathbf{x})$$

where  $\mathbf{p}_i$  is the  $i^{th}$  mesh nodes,  $\varphi_i(\cdot)$  is the  $i^{th}$   $\mathbb{P}^2$  Lagrange shape function defined by :

$$\begin{cases} \varphi_i(\mathbf{x}) = \psi_i(\mathbf{x})(2\psi_i(\mathbf{x}) - 1), & i = 1, 2, 3 \\ \varphi_i(\mathbf{x}) = 4\psi_{[i]}(\mathbf{x})\psi_{[i+1]}(\mathbf{x}), & i = 4, 5, 6 \text{ (edges midpoints)} \end{cases}$$

and  $\psi_i$  is the  $i^{th}$   $\mathbb{P}^1$  Lagrange shape function defined by :

$$\psi_i(\mathbf{p}_j) = \delta_{ij}, \quad \mathbf{p}_j \in \mathcal{H}.$$

We approximate the local interpolation error  $\mathbf{e}_h = |u - \Pi_h^2 u|$  by an homogeneous polynomial of degree  $k = 3$  in 2 variables :

$$P_e(\mathbf{x}) = \sum_{i=0}^k \binom{k}{i} a_i x^i y^{k-i}. \quad (1)$$

$\binom{k}{i}$  are the binomial coefficients and  $a_i$  are the third-order derivatives of  $u$  on each vertex of the mesh. When  $u$  is a numerical solution, they are obtained by using a reconstruction method based on the Clément interpolation operator.

To recover the third-order derivatives  $D_R^{(3)}u$ , the process starts from the constant Hessian  $Hu|_K$  on  $K$  given by :

$$Hu|_K(\mathbf{x}) = \sum_{i=1}^6 u(\mathbf{p}_i) H\varphi_i(\mathbf{x}).$$

For each  $\mathbf{p}_i$ , we thus have the following Hessian reconstruction :

$$H_Ru(\mathbf{p}_i) = \frac{\sum_{K_j \in S_i} |K_j| Hu|_{K_j}}{|S_i|}, \quad (2)$$

where  $|K_j|$  denote the area of  $K_j$  and  $S_i$  the area of the stencil of  $\mathbf{p}_i$ . To recover the third-order derivatives  $a_i = [D_R^{(3)}]_i$  from  $u$ , we apply a gradient reconstruction procedure to each component of the Hessian.

$$D_R^{(3)}u(\mathbf{p}_i) = \frac{\sum_{K_j \in S_i} |K_j| \nabla(H_Ru)|_{K_j}}{|S_i|}. \quad (3)$$

## 2 Local error decomposition and optimal local metric

In this section, we approach locally the variations of  $P_e$  by a quadratic definite positive form (a metric tensor) taken at power  $\frac{k}{2}$ , i.e, for  $\mathbf{x} = (x, y) \in \mathbb{R}^2$ ,

$$|P_e(\mathbf{x})| \leqslant ({}^t\mathbf{x} \mathcal{M}_{opt}^{loc} \mathbf{x})^{\frac{k}{2}}. \quad (4)$$

Geometrically, the local optimal metric is the one of maximal area whose unit ball is included in the isoline 1 of  $|P_e|$ . To obtain  $\mathcal{M}_{opt}^{loc}$ , we propose a local optimization problem based on the Sylvester's theorem [4]. The Sylvester binary decomposition allows to write the 2-dimensional homogeneous polynomial  $P_e(x, y)$  of degree  $k$  as a sum of  $k^{th}$  powers of  $r$  distinct linear forms in  $\mathbb{C}$  :

$$P_e(\mathbf{x}) = \sum_{j=1}^r \lambda_j (\alpha_j x + \beta_j y)^k, \quad (5)$$

$r$  is the decomposition rank, i.e it is the minimal number of linear terms such that (5) holds. We use the algorithm proposed in [4].

Once we obtain the decomposition (5),  $\mathcal{M}_{opt}^{loc}$  is obtained differently according to the nature of the coefficients  $(\alpha_j, \beta_j)$ :

- Real case:  $\mathcal{M}_{opt}^{loc} = {}^tQ \begin{pmatrix} \frac{1}{h_1^2} & 0 \\ 0 & \frac{1}{h_2^2} \end{pmatrix} Q.$
- Complex case:  $\mathcal{M}_{opt}^{loc} = 2^{-\frac{1}{3}} {}^t\bar{Q} \begin{pmatrix} \frac{1}{h_1^2} & 0 \\ 0 & \frac{1}{h_2^2} \end{pmatrix} Q,$

where  $Q = \begin{pmatrix} \alpha_1 & \beta_1 \\ \alpha_2 & \beta_2 \end{pmatrix}$  gives the optimal directions of  $\mathcal{M}_{opt}^{loc}$ .  ${}^tQ$  is the real transpose and  ${}^t\bar{Q}$  is the conjugate complex transpose of  $Q$ . The sizes along optimal directions are:  $h_i = \frac{1}{|\lambda_i|^{\frac{1}{k}}}$ . We depict in Figure 1 two error models and their corresponding optimal metric  $\mathcal{M}_{opt}^{loc}$ .

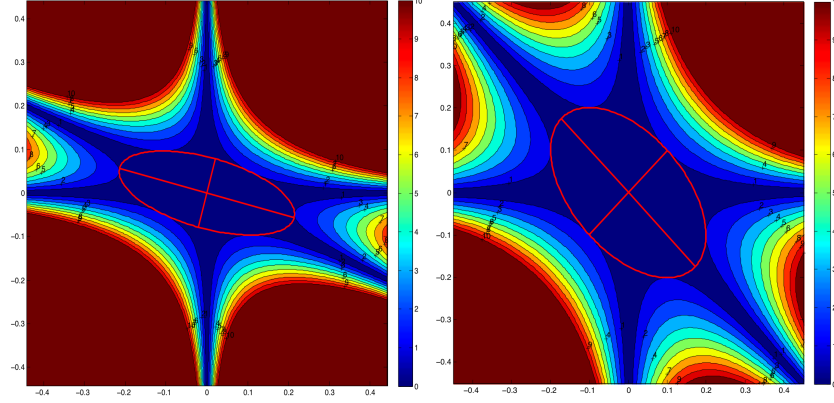


**Fig. 1.** Examples of error models :  $P_e = 50x^3 - 120x^2y - 1000xy^2 - y^3$  (left),  $P_e = x^3 - 500x^2y - 500xy^2 - y^3$  (right). Representation of their iso-values and their corresponding optimal ellipse included in the isoline 1(in red).

### 3 Global variational calculus problem

The global optimal continuous metric  $\mathbf{M}_{\mathbf{L}^p}^N = (\mathcal{M}_{\mathbf{L}^p}^N(\mathbf{x}))_{\mathbf{x} \in \mathbb{R}^2}$  is the solution of the following variational calculus problem written in  $\mathbf{L}^p$  norm:

$$\mathbf{M}_{\mathbf{L}^p}^N = \min_{\mathbf{M}} E_p(\mathbf{M}) = \left( \int_{\Omega} |e_{\mathcal{M}}(\mathbf{x})|^p d\mathbf{x} \right)^{\frac{1}{p}} = \left( \int_{\Omega} |{}^t\mathbf{x} \mathcal{M}(\mathbf{x}) \mathbf{x}|^{\frac{kp}{2}} d\mathbf{x} \right)^{\frac{1}{p}} \quad (6)$$

under the constraint  $\mathcal{C}(\mathbf{M}) = \int_{\Omega} (h_1 h_2)^{-1} = N$ . To solve this problem, we use the Euler-Lagrange necessary condition which states that there exists  $\alpha$  a constant such that  $\forall \delta \mathcal{M}, \delta E(\mathbf{M}, \delta \mathbf{M}) = \alpha \delta \mathcal{C}(\mathbf{M}, \delta \mathbf{M})$ .  $\mathbf{M}_{\mathbf{L}^p}^N$  writes:

$$\mathbf{M}_{\mathbf{L}^p}^N = N \left( \int_{\Omega} (\lambda_1 \lambda_2)^{\frac{kp}{2(kp+2)}} \right)^{-1} (\lambda_1 \lambda_2)^{-\frac{1}{kp+2}} \begin{pmatrix} \lambda_1 & 0 \\ 0 & \lambda_2 \end{pmatrix}.$$

The optimal value of the density is :

$$d_{\mathbf{L}^p}^N = N \left( \int_{\Omega} (\lambda_1 \lambda_2)^{\frac{kp}{2(kp+2)}} \right)^{-1} (\lambda_1 \lambda_2)^{\frac{kp}{2(kp+2)}},$$

and the optimal value of the error is:

$$E_p(\mathbf{M}_{\mathbf{L}^p}^N)^p = 2^{\frac{k}{2}} N^{-\frac{k}{2}} \left( \int_{\Omega} (\lambda_1 \lambda_2)^{\frac{kp}{2(kp+2)}} \right)^{\frac{k}{2}} (\lambda_1 \lambda_2)^{\frac{k}{2(kp+2)}}.$$

The order of convergence for a sequence of continuous meshes  $(\mathcal{M}_{\mathbf{L}^p}^N)_N$  verifies:

$$\|u - \Pi_{\mathcal{M}_{\mathbf{L}^p}^N}^2 u\|_{\mathbf{L}^p(\Omega)} \leq \frac{Cst}{N^{\frac{k}{2}}}. \quad (7)$$

Relation (7) points out a global  $k$ th-order of spatial mesh convergence.

## 4 Numerical example

To validate our approach, we compare an adaptation based on the previous optimal metric (with third order derivatives recovery) with an adaptation only based on the Hessian on  $u$  (constant by triangles). For both strategies, the interpolation error level is computed by mean of 5th order gauss interpolation to estimate  $\|u - \Pi_h^2 u\|_{\mathbf{L}^p(\Omega)}$ . Consequently, we compare a  $\mathbb{P}^1$ -driven adaptation with a  $\mathbb{P}^2$ -driven adaptation having a  $\mathbb{P}^2$ -Lagrange triangle to represent the function. We consider:

$$f(x, y) = \begin{cases} 0.01 \sin(50xy) & \text{if } xy \leq -\frac{\pi}{50} \\ \sin(50xy) & \text{if } -\frac{\pi}{50} < xy \leq \frac{2\pi}{50} \\ 0.01 \sin(50xy) & \text{if } xy > \frac{2\pi}{50} \end{cases}$$

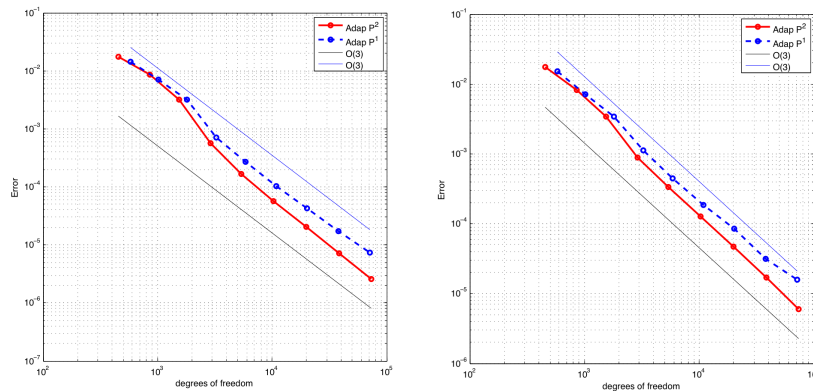


**Fig. 2.** Convergence curves :  $\mathbf{L}^1$  norm of the error versus the number of dof (left),  $\mathbf{L}^2$  norm of the error versus the number of dof (right) for the function  $f$ .

The spatial convergence curves are depicted in Figure 2 and the meshes in Figure 3. The sequence of  $\mathbb{P}^2$ -driven adapted mesh shows a 3rd order of convergence while  $\mathbb{P}^1$ -driven adaptation shows an asymptotic rate of convergence

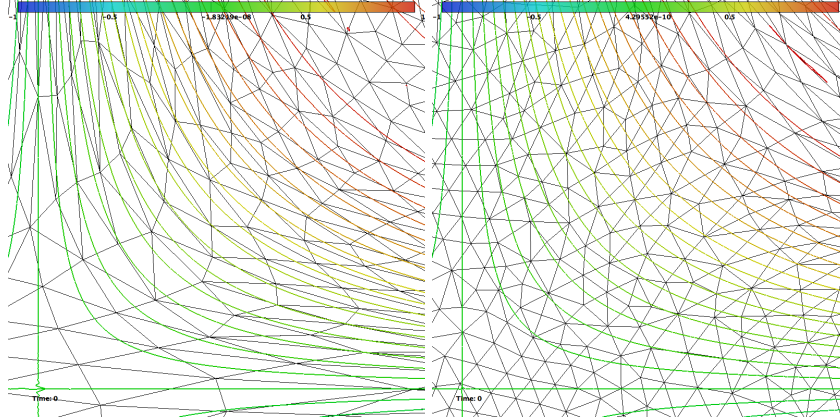


**Fig. 3.** Closer view of the meshes obtained for a  $\mathbb{P}^2$ -driven adaptation (left) and  $\mathbb{P}^1$ -driven adaptation (right) for  $f$ . Both meshes contains around 42 000 dofs.

of one (despite the interpolation is still 2nd order) for  $\mathbf{L}^1$  and  $\mathbf{L}^2$  norms. This emphasizes the needs to consider higher-order interpolation error in order to achieve an optimal rate of convergence.

## 5 Conclusion

We have shown that anisotropic mesh adaptation can be extended to higher order interpolations. We are currently extending this approach to the 3 dimensional case by using tensor decomposition methods. Extension to curved isoparametric triangles is also ongoing.

## References

1. A. Loseille, F. Alauzet : Continuous mesh framework, Part I: well-posed continuous interpolation error and Part II: validations and applications, SIAM in Numerical Analysis, Vol. 49, Issue 1, 2011.
2. W. Cao : An interpolation error estimate on anisotropic meshes in  $R^n$  and optimal metrics for mesh refinement, SIAM in Numerical Analysis, Vol. 45 (2007), no. 6, 2368-2391.
3. J.-M.Mirebeau : Optimal meshes for finite elements of arbitrary order, Springer Science+Business Media,LLC 2010, 18 February 2010.
4. P. Comon, B. Mourrain : Decomposition of quantics in sums of powers of linear forms, February 1999.